J Biomol NMR (2012) 52:31–39
DOI 10.1007/s10858-011-9591-4

ARTICLE

Assignment strategies for aliphatic protons in the solid-state in randomly protonated proteins

Sam Asami · Bernd Reif

Received: 10 July 2011 / Accepted: 25 September 2011 / Published online: 4 December 2011

Abstract Biological solid-state nuclear magnetic resonance spectroscopy developed rapidly in the past two decades and emerged as an important tool for structural biology. Resonance assignment is an essential prerequisite for structure determination and the characterization of motional properties of a molecule. Experiments, which rely on carbon or nitrogen detection, suffer, however, from low sensitivity. Recently, we introduced the RAP (Reduced Adjoining Protonation) labeling scheme, which allows to detect backbone and sidechain protons with high sensitivity and resolution. We present here a ^{1}H-detected 3D (H)CCH experiment for assignment of backbone and sidechain proton resonances. Resolution is significantly improved by employing simultaneous ^{13}CO and ^{13}Cβ *J*-decoupling during evolution of the ^{13}Cα chemical shift. In total, $\sim$90% of the ^{1}Hα-^{13}Cα backbone resonances of chicken α-spectrin SH3 could be assigned.

Keywords Magic angle spinning (MAS) solid-state NMR · Perdeuteration · 2H-labeling · Side chain assignment strategies

Introduction

Solid-state NMR spectroscopy has rapidly developed over the past few years, facilitating structural studies on crystalline (Castellani et al. 2002; Franks et al. 2008; Zech et al. 2005) and non-crystalline systems (Ferguson et al. 2006; Jaroniec et al. 2002; Wasmer et al. 2008). Traditionally, solid-state NMR spectroscopy relies on the detection of ^{13}C and ^{15}N heteronuclei, which compromises sensitivity due to their low gyromagnetic ratios. Theoretically, direct ^{1}H-detection yields a gain in sensitivity by a factor of 8 and 31, compared to ^{13}C and ^{15}N detection, respectively. In uniformly protonated protein samples, the proton resonances are largely broadened due to ^{1}H,^{1}H dipolar couplings. Employing homonuclear decoupling sequences, proton linewidths of about 100–500 Hz can be achieved (Bielecki et al. 1989; Bosman et al. 2004; Levitt et al. 1993; Sakellariou et al. 2000; Vinogradov et al. 1999). Partial or full deuteration of a protein decreases the ^{1}H dipolar network and increases the coherence lifetimes (Garrett et al. 1997; Kalbitzer et al. 1985; Lemaster and Richards 1988).

In the solid-state, the proton linewidth of exchangeable protons can amount to 20-40 Hz in case heavily deuterated samples are employed (Agarwal et al. 2006; Akbey et al. 2010; Asami et al. 2010; Chevelkov et al. 2006; Schanda et al. 2009). Methyl protons are accessible by making use of specific precursors for amino acid biosynthesis (Agarwal et al. 2006, 2008), or by exploiting the fact that commercially available precursors are typically not 100% enriched in deuterium (Agarwal and Reif 2008). The deuteration

Electronic supplementary material The online version of this article (doi:10.1007/s10858-011-9591-4) contains supplementary material, which is available to authorized users.

S. Asami · B. Reif (✉)
Leibniz-Institut für Molekulare Pharmakologie (FMP), Robert-Rössle-Straße 10, 13125 Berlin, Germany
e-mail: reif@tum.de

B. Reif
Department of Chemistry (CIPS-M), Munich Center for Integrated Protein Science, Technische Universität München (TUM), Lichtenbergstr. 4, 85747 Garching, Germany

B. Reif
Helmholtz-Zentrum München (HMGU), Deutsches Forschungszentrum für Gesundheit und Umwelt (HMGU), Ingolstädter Landstr. 1, 85764 Neuherberg, Germany

scheme is not only applicable to microcrystalline proteins, but is also successfully implemented in amyloid fibrils and membrane proteins (Linser et al. 2011).

Aliphatic resonances are essential to access tertiary structure information of a protein, since long-range restraints between sidechains are fundamental for defining the tertiary structure of a protein (Gardner et al. 1997; Huber et al. 2011; Liu et al. 1992; Zwahlen et al. 1998). In uniformly protonated samples ^{1}H,^{1}H long-range restraints can be determined using XHHY (X,Y = ^{13}C, ^{15}N) type experiments using spin diffusion for mixing of magnetization (Lange et al. 2002; Reif et al. 2003). These experiments, however, suffer from low sensitivity due to the detection of low-γ nuclei. In the solid-state, highly resolved deuterium spectra can be recorded yielding chemical shift information at aliphatic sites (Agarwal et al. 2009). Due to dipolar truncation effects, this labeling scheme is, however, not suitable to deliver long-range structural information.

Recently, we introduced the RAP (Reduced Adjoining Protonation) labeling scheme, which yields randomly protonated samples in a deuterated matrix (Asami et al. 2010). The degree of protonation can be adjusted by the relative amount of H_2O in the M9 growth medium. This scheme enables the determination of long-range ^{1}H,^{1}H distance restraints. Dipolar truncation effects are avoided due to the statistical distribution of protons in the protein. Assignments are essential to proceed with investigations of structure and dynamics. For methyl groups, we proposed recently a ^{1}H-detected out-and-back (H)CCH-TOBSY experiment (Agarwal and Reif 2008), which employs refocused INEPT transfers in combination with ^{13}C homonuclear mixing. Due to the intrinsically short ^{13}Cα-T_2 coherence lifetimes at moderate rotation frequencies (H)CCH-TOBSY type experiments are not suitable for the assignment of ^{1}Hα,^{13}Cα cross peaks. Furthermore, ^{1}Hα,^{13}Cα backbone assignments are complicated due to artifacts, which arise from the residual solvent signal. In this manuscript, we present 3D HCC and CCH type correlation experiments which allowed us to assign $\sim$90% of the ^{1}Hα,^{13}Cα backbone resonances of a 15% RAP sample of the chicken α-spectrin SH3 domain. Generally, ^{13}Cα resonances in uniformly ^{13}C-labeled proteins are broadened due to the evolution of J-couplings to ^{13}CO and ^{13}Cβ nuclei, except in the case of glycines, which lack carbon sidechains. We show, that ^{13}C-^{13}C J-decoupling sequences applied during the ^{13}Cα evolution period yields a dramatically improved resolution in ^{1}Hα,^{13}Cα correlation experiments.

Materials and methods

Sample preparation

For the presented studies, randomly protonated α-spectrin SH3 was produced as described earlier (Asami et al. 2010; Chevelkov et al. 2006). In brief, SH3 was expressed in M9 minimal medium employing $^{15}NH_4Cl$ and u-[^{13}C,^{2}H] glucose. The nutrients were dissolved in buffer containing 15% H_2O and 85% D_2O. In the following, this sample is referred to as a 15% RAP sample. Two samples were crystallized from this material, containing 10% H_2O/90% D_2O and $\sim$0% H_2O/100% D_2O in the crystallization buffer, respectively. In addition, 75 mM Cu(II)-EDTA was added to reduce the recycle delay of the experiments (Linser et al. 2007; Wickramasinghe et al. 2009). For each sample, approximately 15 mg of protein was packed into a 3.2 mm rotor.

NMR spectroscopy

The NMR experiments were carried out on a Bruker Biospin Avance spectrometer operating at ^{1}H Larmor frequencies of 600 and 700 MHz, using a commercial 3.2 mm triple-resonance probe. Experiments, recorded at 600 MHz, were performed by setting the MAS rotation frequency to 24 kHz. The effective sample temperature was adjusted to $\sim$20 to 24°C. Experiments carried out at 700 MHz were recorded by setting the MAS rotation frequency to 18 kHz. In this case, the effective sample temperature was set to $\sim$13 to 17°C. In all experiments, cross polarization (CP) is employed for magnetization transfer.

For ^{13}CO + ^{13}Cβ homonuclear scalar decoupling, adiabatic HS2 inversion pulses were employed during the ^{13}Cα evolution period (Hennig et al. 2000). The HS2 inversion pulses, which had a pulse length of 4 ms, were applied continuously throughout the whole indirect evolution period, using a (p5) (m4) phase cycle (Fig. 1a). The experimental inversion profile of the HS2 shape is shown in Fig. 1b. Thr-^{13}Cβ resonances are downfield shifted with respect to Thr-^{13}Cα and resonate outside the inversion region of the utilized adiabatic inversion pulse. For ^{1}H,^{13}C correlation experiments, acquisition times of 83, 26.5 ms (52, 14.2 ms) in the direct ^{1}H- and the indirect ^{13}C-dimension were employed. Values in parentheses indicate the acquisition times in absence of ^{13}CO + ^{13}Cβ J-decoupling. The recycle delay in both experiments was set to 0.8 s. Water suppression was achieved employing the MISSISSIPPI scheme (Zhou and Rienstra 2008).

The ^{13}C- and ^{1}H-excited ^{13}C,^{13}C correlation experiments were recorded, employing adiabatic RFDR for ^{13}C,^{13}C mixing (Leppert et al. 2003), using a mixing time of 9.9 ms with t_1^{max} = 4.3 ms and a recycle delay of 3 s. The same settings for homonuclear mixing were employed to acquire the ^{1}H- and ^{13}C-detected 3D CCH and HCC experiments. Cross polarization employing rf fields on two or three channels (^{1}H,^{13}C and ^{1}H + ^{2}H,^{13}C), are referred to as 2CP and 3CP, respectively. The CP contact time for 2CP and 3CP was 1 ms, with a ^{13}C rf field of 24 kHz and a ^{1}H rf

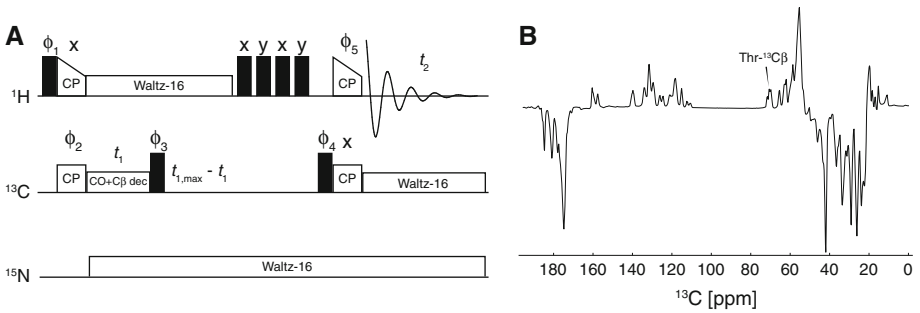

Fig. 1 **a** ^{1}H-detected 2D (H)CH experiment with ^{13}CO + ^{13}Cβ-decoupling. Water suppression was achieved with a constant-time MISSISSIPPI sequence. ϕ_1 = (y, −y), ϕ_2 = (x, x, −x, −x), ϕ_3 = (y), ϕ_4 = (y), ϕ_5 = (x, x, x, x, −x, −x, −x, −x), ϕ_{rec} = (y, −y, −y, y), (−y, y, y, −y). **b** Inversion profile of the utilized adiabatic HS2 pulse

field strength ramped linearly around the $n = 1$ Hartmann-Hahn matching condition. The MAS frequency was set to 18 kHz. The ^{2}H rf field for ^{2}H,^{13}C CP was ramped between 38 and 59 kHz (n = 2–3). Experimentally, it was found, that ^{2}H,^{13}C CP sensitivity benefits from high power levels, especially for the backbone resonances, even though spinning sidebands with $n > 1$ are matched. However, with the available rf power on the ^{2}H channel the whole ^{2}H spectrum cannot be excited and using maximum power to achieve a $n = 1$ condition might damage the probe. The 2CP and 3CP experiments were carried out using a 600 MHz spectrometer.

In the 3D CCH experiment, acquisition times of 36.4, 8.1 and 4.6 ms were employed in the direct ^{1}H-dimension (ω_3) and the indirect ^{13}C-dimensions (ω_2) and (ω_1). ^{13}C excitation is facilitated by paramagnetic doping to reduce the recycle delay. This way, the T_1 relaxation time of the bulk ^{13}Cα magnetization can be reduced to ~3.5 s. Use of a recycle delay of 1 s allows to select for methylene and methyl resonances. The 3D HCC experiment was acquired using acquisition times of 11.5, 4.9 and 5.1 ms in the direct ^{13}C-dimension (ω_3) and the indirect ^{1}H- and ^{13}C-dimension (ω_1, ω_2). The recycle delay was set to 0.6 s. To record the ^{13}C-detected 3D HCC assignment experiment, a sample was used, which was prepared using 10% H_2O and 90% D_2O in the crystallization buffer. For the ^{1}H-detected 3D CCH experiment, a sample crystallized from 100% D_2O was employed. In all experiments, 2–3 kHz low-power WALTZ-16 (Shaka et al. 1983) decoupling was used. Quadrature detection was achieved using TPPI (Marion and Wuthrich 1983).

Results and discussion

Resolution enhancement of 2D ^{1}Hα,^{13}Cα correlations

Figure 2 shows 2D ^{1}Hα,^{13}Cα correlations obtained for a 15% RAP sample of α-spectrin SH3. To yield optimal water suppression, the ^{13}C evolution period was designed in a constant-time fashion (Paulson et al. 2003). In the absence of homonuclear decoupling, the ^{1}Hα,^{13}Cα region of the spectrum is rather poorly resolved, yielding ^{13}Cα linewidths on the order of 105 Hz. ^{13}CO,^{13}Cα and ^{13}Cβ,^{13}Cα scalar couplings, which are on the order of 55 and 35 Hz, respectively, contribute significantly to the broadening of the ^{13}Cα resonances. To improve the resolution in the ^{1}Hα,^{13}Cα spectral region, we employed

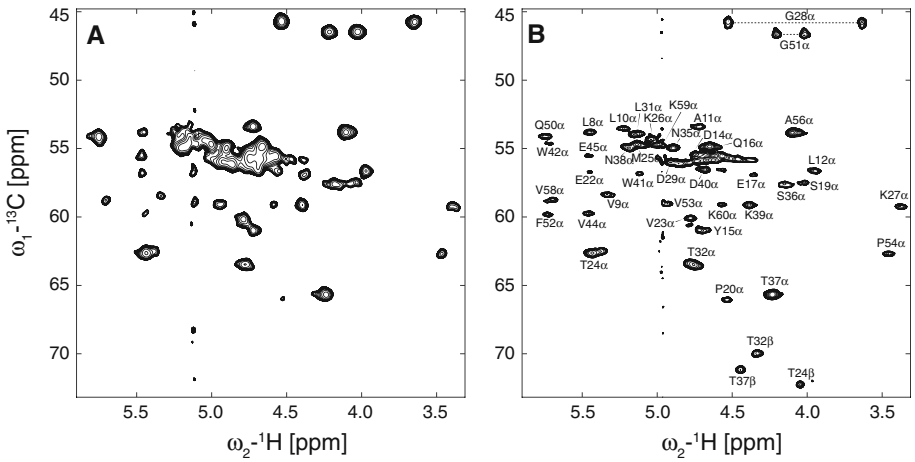

Fig. 2 ^{1}Hα,^{13}Cα correlation spectra of a 15% RAP sample of α-spectrin SH3. **a** Without and **b** with ^{13}CO + ^{13}Cβ homonuclear scalar decoupling during ω_1, employing the pulse sequence shown in Fig. 1a. The spectra were recorded at 600 MHz, setting the MAS rotation frequency to 24 kHz

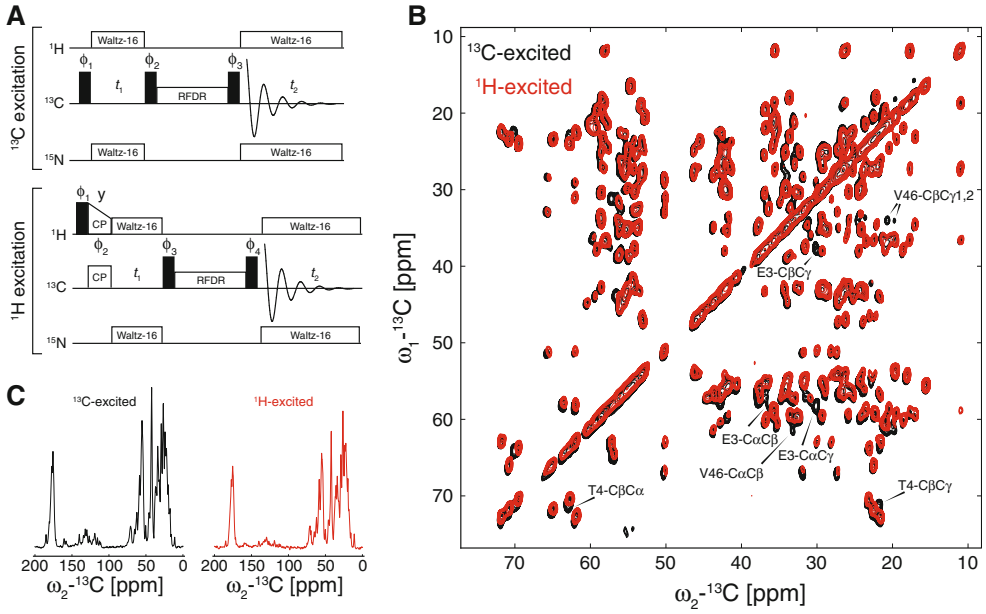

Fig. 3 ^{13}C- versus ^{1}H-excitation in a 15% RAP sample of α-spectrin SH3. **a** ^{13}C-excited experiment: $\phi_1 = (-x, x)$, $\phi_2 = (x)$, $\phi_3 = (-x, -x, x, x)$, $\phi_{rec} = (-x, x, x, -x)$. ^{1}H-excited experiment: $\phi_1 = (-x, x)$, $\phi_2 = (y, y, y, y, -y, -y, -y, -y)$, $\phi_3 = 8(x), 8(-x)$, $\phi_4 = (-x, -x, x, x)$, $\phi_{rec} = (-x, x, x, -x), 2(x, -x, -x, x), (-x, x, x, -x)$. **b** Superposition of a ^{13}C- (*black*) and ^{1}H- (*red*) excited ^{13}C-^{13}C RFDR spectrum. Missing peaks in the ^{1}H-excited spectrum are labeled with their respective assignment. **c** First increments of the ^{13}C- and ^{1}H-excited experiment. Both spectra were recorded with the same number of scans and recycle delay

adiabatic HS2 inversion pulses during the ^{13}Cα evolution period (Fig. 1a). The enhancement of the resolution can be clearly appreciated from Fig. 2b. The linewidths can be reduced to 35–60 Hz. Alternatively, a constant-time experiment (Vuister and Bax 1992) can be carried out to yield a similar improvement in resolution. In the absence of high-power proton decoupling and at the moderate rotation frequencies employed in this study, backbone coherence lifetimes are short and constant-time experiments are too insensitive.

Proton versus carbon excitation

We designed backbone assignment experiments utilizing both proton and carbon excitation. Proton excitation is in principle more favorable due to the higher gyromagnetic ratio of protons and their shorter T_1 relaxation times. However (H)CCH experiments are not easily feasible as protons are randomly distributed in RAP samples. In a 15% RAP sample, approximately 17% of all Cα carbons, and 10–16% of the sidechain carbons are protonated (Asami et al. 2010). To probe whether proton or carbon excitation is more favorable, we compare in the following the sensitivity of ^{1}H- and ^{13}C-excited 2D ^{13}C,^{13}C RFDR experiments (Fig. 3a). In RAP samples (in contrast to perdeuterated samples), uniform excitation of all sidechain carbons is not an issue due to a more or less isotropic incorporation of protons in all positions. In the ^{1}H-excited experiment, approximately the same number of correlations is observable (Fig. 3b). Missing peaks originate from residues located at the flexible N-terminus or in loop regions (e.g. V46). These residues are mobile and magnetization is not transferred by cross polarization.

Both RFDR experiments, ^{1}H- and ^{13}C-excited, were recorded with a recycle delay of 3 s and the same number of scans. The first increment of the two experiments yields rather similar intensities (Fig. 3c). Note that the recycle delay for the ^{1}H-excited RFDR experiment can be reduced to ~0.5 s, since the apparent T_1 time for protons is much shorter than for carbons. Thus, the ^{1}H-excited experiment yields an approximately ~2.5× larger sensitivity (per unit time) in comparison to the ^{13}C-excited experiment.

To further increase the achievable sensitivity, the ^{1}H,^{13}C cross polarization transfer step (2CP, Fig. 4a, left) was supplemented with a 90° ^{13}C pulse for direct carbon excitation and an additional ^{2}H,^{13}C transfer step (3CP, Fig. 4a, right). Employing 3CP yields a gain in the signal-to-noise ratio for the ^{13}Cα region of approximately a factor of 1.6 (Fig. 4b). A similar observation was reported recently for uniformly deuterated and ^{1}H back-exchanged samples (Akbey et al. 2011). In this context, a four channel probe with high-power capabilities for ^{1}H, ^{2}H, ^{13}C and low-power capabilities for ^{15}N would be desirable. Simultaneous cross polarization among ^{1}H, ^{13}C and ^{2}H, in combination with scalar decoupling in the direct and indirect evolution periods (Fig. 4c) would yield another increase in performance. The use of Optimum Control (OC) in pulse sequence design might further allow to

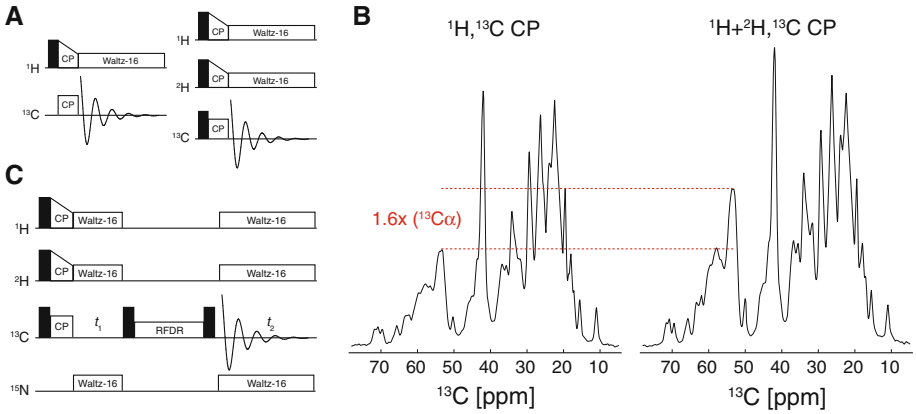

Fig. 4 Simultaneous $^{1}H + {}^{2}H,{}^{13}C$ cross polarization (3CP) yields a significant improvement in sensitivity. **a** Pulse scheme for the $^{1}H,{}^{13}C$ 2CP (left) and $^{1}H + {}^{2}H,{}^{13}C$ 3CP (right) experiment. **b** Comparison of the sensitivity of 2CP and 3CP experiments. **c** 3CP ^{13}C-^{13}C RFDR pulse sequence for a 4-channel probe

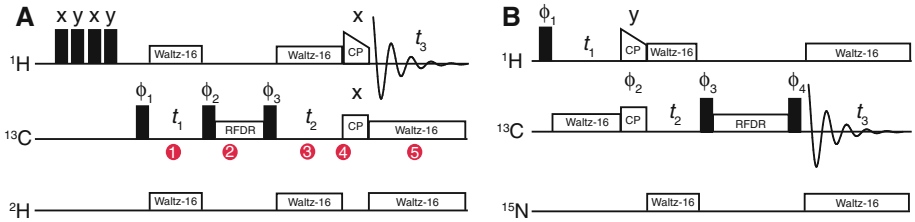

Fig. 5 3D CCH and HCC experiments for assignment of aliphatic resonances in RAP labeled protein samples. **a** ^{1}H-detected, $\phi_1 = (y, -y)$, $\phi_2 = (y)$, $\phi_3 = (y, y, -y, -y)$, $\phi_{rec} = (y, -y, -y, y)$. **b** ^{13}C-detected, $\phi_1 = (-x, x)$, $\phi_2 = 4(y), 4(-y)$, $\phi_3 = 8(x), 8(-x)$, $\phi_{rec} = (-x, x, x, -x), 2(x, -x, -x, x), (-x, x, x, -x)$

improve sensitivity by reducing the required rf fields on the ^{2}H channel (Wei et al. 2011).

Assignment of $^{1}H\alpha,{}^{13}C\alpha$ backbone correlations

To assign the $^{1}H\alpha,{}^{13}C\alpha$ backbone region, we performed a ^{1}H-detected 3D CCH correlation experiment which is represented in Fig. 5a. In this experiment, the $^{1}H\alpha$ chemical shift is correlated with the chemical shift of the directly bound $^{13}C\alpha$ carbon, and after a homonuclear mixing step, with the chemical shift of $^{13}CO/{}^{13}C\beta$. The experiment allows to assign backbone as well as sidechain resonances. All expected ^{13}C resonances throughout the whole sidechain could be detected (Fig. 6a). Figure 6b relates schematically the different stages of the pulse scheme in Fig. 5a to the molecular frame, employing the amino acid lysine as an example. In the proton detected experiment, observation of the $^{1}H\alpha,{}^{13}C\alpha$ correlations is complicated due to solvent suppression artifacts. These difficulties might be overcome as soon as pulsed field gradients become routinely available for MAS solid-state NMR applications (Chevelkov et al. 2003).

In case water suppression is an issue, a ^{13}C-detected HCC experiment can be recorded, employing the pulse scheme shown in Fig. 5b. The sequence starts out with an indirect proton evolution period $\omega_1(^{1}H)$. Magnetization is transferred then via cross polarization to carbons, followed by a first ^{13}C evolution period $\omega_2(^{13}C)$. After $^{13}C,{}^{13}C$ homonuclear mixing, the carbon signal is detected in a second ^{13}C dimension $\omega_3(^{13}C)$, facilitating unambiguous resonance assignments. Heteronuclear scalar decoupling is achieved by application of low-power WALTZ-16 (Shaka et al. 1983) employing an rf field strength on the order of 2–3 kHz. In total, 45 of 51 possible $^{1}H\alpha,{}^{13}C\alpha$ backbone resonances (~90%) were unambiguously assigned. Representative strips from this experiment are depicted in Fig. 7. Assignments obtained this way are employed to annotate Fig. 2b. A table with the experimental $^{1}H\alpha$ and $^{13}C\alpha$ chemical shifts is given as part of the Supporting Information. Since this second sample contained approximately 10% protons at exchangeable sites, most of the $^{1}H^{N}$ chemical shifts could be assigned as well (Fig. 7). Correlations between $^{1}H^{N}$ and $^{13}C\alpha/{}^{13}CO$ are due to long-range through-space connectivities (Agarwal et al. 2010).

In the ^{13}C-detected HCC experiment, the Hartmann-Hahn matching condition during the cross polarization transfer step (Fig. 5b) was optimized to yield maximum sensitivity for aliphatic resonances and minimum intensity for ^{13}CO (Baldus et al. 1998; Laage et al. 2008). This way, the spectral width in the $\omega_2(^{13}C)$ dimension could be reduced to 70 ppm suppressing at the same time folding artifacts from ^{13}CO resonances. In case the experiment

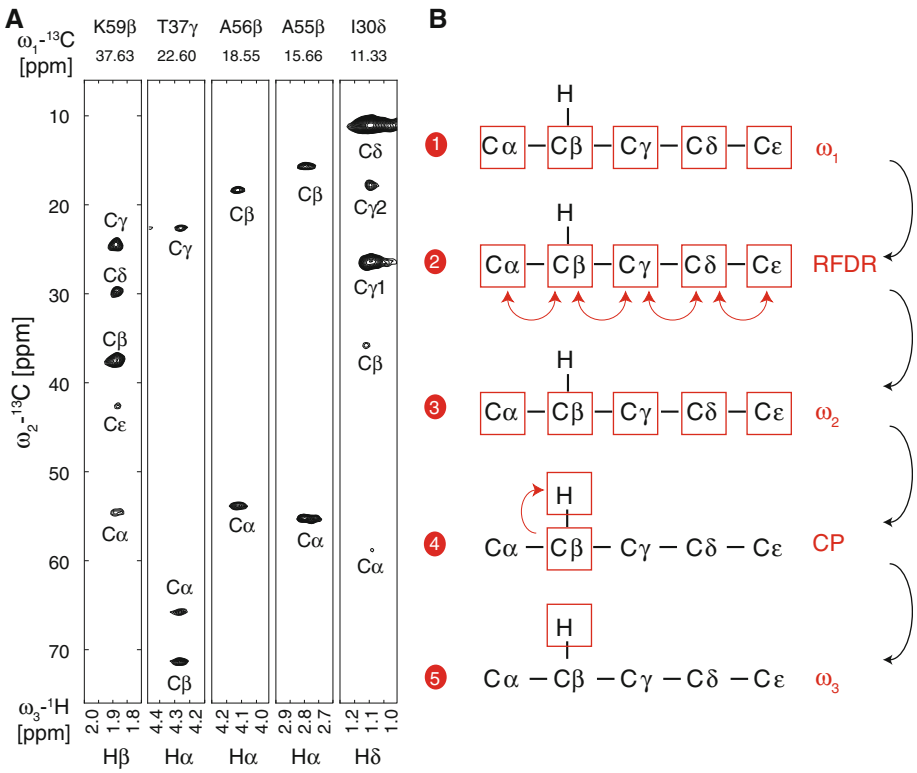

Fig. 6 **a** 2D strips extracted from the ^{1}H-detected, ^{13}C-excited 3D CCH correlation experiment. The assignments on the top and at the bottom of the strips indicate the carbon and proton nuclei, which are evolving during t_1 and t_3, respectively. All expected intraresidual correlations are observed. **b** Schematic representation of lysine, highlighting the distribution of magnetization at the different stages of the pulse scheme from Fig. 5a

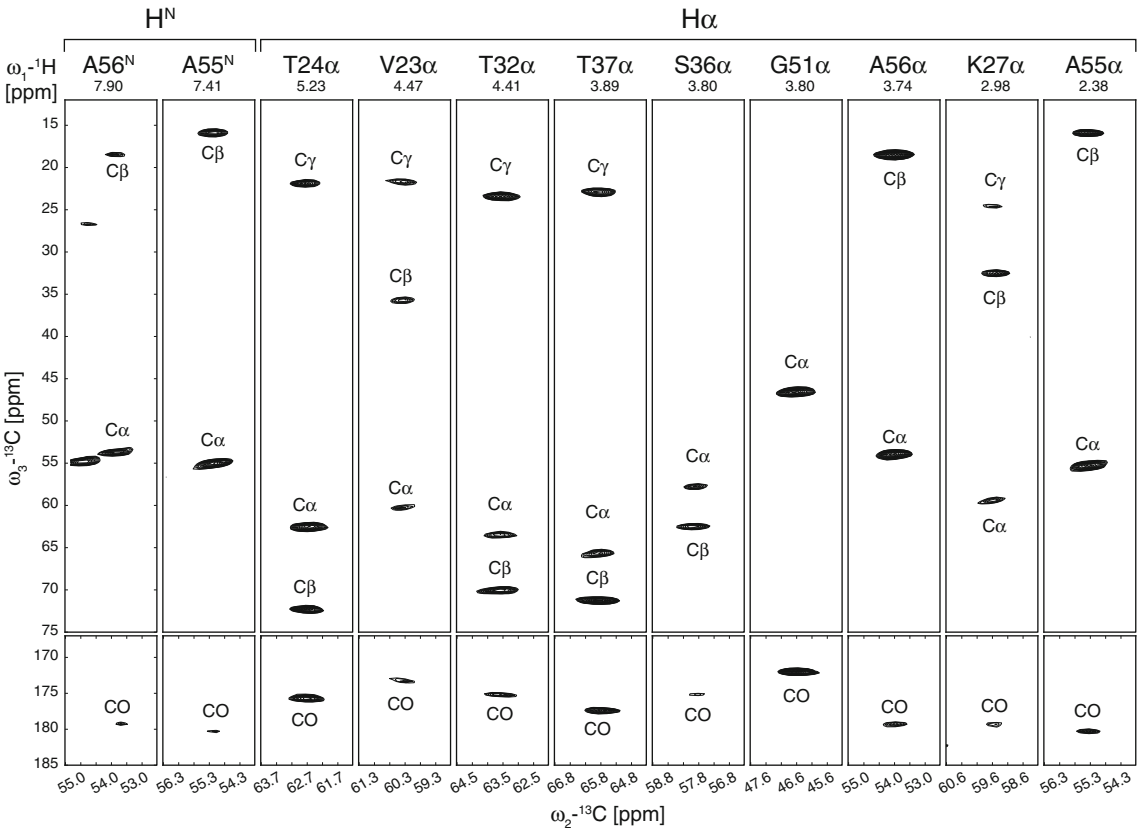

Fig. 7 2D strips extracted from the ^{13}C-detected 3D HCC correlation experiment recorded for the α-spectrin SH3 domain. ^{1}H^{N} as well as ^{1}Hα chemical shifts can be unambiguously assigned by correlating ^{13}Cα to ^{13}Cβ/^{13}CO chemical shifts. Note that the direct dimension ω_3(^{13}C) is represented as the vertical dimension

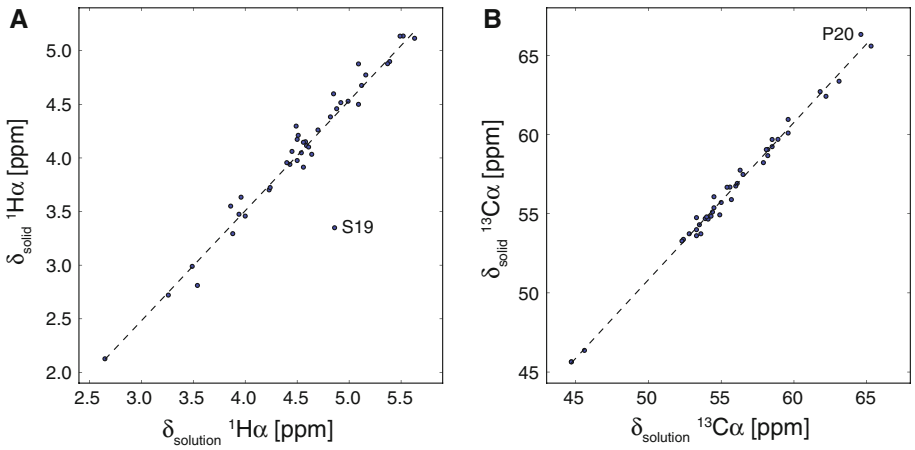

Fig. 8 Correlation diagram of solution-state versus solid-state NMR chemical shifts for **a** ^{1}Hα and **b** ^{13}Cα in α-spectrin SH3

would be recorded in such a way that magnetization transfer to ^{13}CO is optimized, sequential assignments via $^{1}H^{N}_{(i)}$–$^{13}C\alpha_{(i)}$ and $^{1}H^{N}_{(i)}$–$^{13}CO_{(i-1)}$ correlations would be obtained. This experiment is superior in terms of sensitivity in comparison to the HNCACX experiments as it lacks the magnetization transfer step to $^{15}N_{(i)}$. Alternatively, amide protons in RAP samples can be assigned using HNCA or HNCACB experiments (Linser et al. 2008), or a combination of 3D HNCO and HNCACO experiments (Linser et al. 2010).

In Fig. 8, the α-spectrin SH3 backbone chemical shifts obtained in the solid-state are compared with the shifts found in solution at pH 7.3 (van Rossum et al. 2001). Both, ^{1}Hα and ^{13}Cα, are well correlated yielding a Spearman's correlation coefficient of 0.909 and 0.991 for ^{1}Hα and ^{13}Cα, respectively. This shows, that the SH3 protein structure in the crystal and in solution are highly similar. Small chemical shift differences arise from residues, which are involved in crystal contacts. In particular, we find deviations from an ideal correlation for the ^{1}Hα-shift of S19 and the ^{13}Cα-shift of P20. These residues are within 6 Å to the aromatic rings of Y13 and Y57 of a molecule in a symmetry related unit cell.

Conclusion

We have shown that the resolution of ^{1}Hα,^{13}Cα correlation spectra in RAP samples can be further improved by application of homonuclear $^{13}CO + {}^{13}C\beta$ scalar decoupling sequences during the ^{13}Cα evolution period. We introduced furthermore proton and carbon detected 3D HCC and 3D CCH assignment experiments, which allow to unambiguously assign ^{1}Hα,^{13}Cα cross peaks by correlating the chemical shifts of ^{1}Hα with ^{13}Cα and $^{13}CO/{}^{13}C\beta$. ^{1}H-detected experiments are more favorable in terms of sensitivity, but suffer from insufficient solvent suppression. We expect that this problem will be overcome in the future once pulsed field gradient probes will become routinely available.

Acknowledgments This research was supported by the Leibniz-Gemeinschaft, the Helmholtz-Gemeinschaft and the DFG (Re1435, SFB449, SFB740). We are grateful to the Center for Integrated Protein Science Munich (CIPS-M) for financial support. We thank W. Bermel for providing Bruker shaped files for scalar homonuclear carbon decoupling.

References

Agarwal V, Reif B (2008) Residual methyl protonation in perdeuterated proteins for multi-dimensional correlation experiments in MAS solid-state NMR spectroscopy. J Magn Reson 194:16–24

Agarwal V, Diehl A, Skrynnikov N, Reif B (2006) High resolution H-1 detected H-1, C-13 correlation spectra in MAS solid-state NMR using deuterated proteins with selective H-1, H-2 isotopic labeling of methyl groups. J Am Chem Soc 128:12620–12621

Agarwal V, Xue Y, Reif B, Skrynnikov NR (2008) Protein side-chain dynamics as observed by solution- and solid-state NMR spectroscopy: a similarity revealed. J Am Chem Soc 130:16611–16621

Agarwal V, Faelber K, Schmieder P, Reif B (2009) High-resolution double-quantum deuterium magic angle spinning solid-state NMR spectroscopy of perdeuterated proteins. J Am Chem Soc 131:2-+

Agarwal V, Linser R, Fink U, Faelber K, Reif B (2010) Identification of hydroxyl protons, determination of their exchange dynamics, and characterization of hydrogen bonding in a microcrystallin protein. J Am Chem Soc 132:3187–3195

Akbey U, Lange S, Franks WT, Linser R, Rehbein K, Diehl A, van Rossum BJ, Reif B, Oschkinat H (2010) Optimum levels of exchangeable protons in perdeuterated proteins for proton detection in MAS solid-state NMR spectroscopy. J Biomol NMR 46:67–73

Akbey U, Camponeschi F, van Rossum BJ, Oschkinat H (2011) Triple resonance cross-polarization for more sensitive (13)C MAS NMR spectroscopy of deuterated proteins. ChemPhysChem 12:2092–2096

Asami S, Schmieder P, Reif B (2010) High resolution H-1-detected solid-state NMR spectroscopy of protein aliphatic resonances: access to tertiary structure information. J Am Chem Soc 132:15133–15135

Baldus M, Petkova AT, Herzfeld J, Griffin RG (1998) Cross polarization in the tilted frame: assignment and spectral simplification in heteronuclear spin systems. Mol Phys 95:1197–1207

Bielecki A, Kolbert AC, Levitt MH (1989) Frequency-switched pulse sequences—homonuclear decoupling and dilute spin NMR in solids. Chem Phys Lett 155:341–346

Bosman L, Madhu PK, Vega S, Vinogradov E (2004) Improvement of homonuclear dipolar decoupling sequences in solid-state nuclear magnetic resonance utilising radiofrequency imperfections. J Magn Reson 169:39–48

Castellani F, van Rossum B, Diehl A, Schubert M, Rehbein K, Oschkinat H (2002) Structure of a protein determined by solid-state magic-angle-spinning NMR spectroscopy. Nature 420:98–102

Chevelkov V, van Rossum BJ, Castellani F, Rehbein K, Diehl A, Hohwy M, Steuernagel S, Engelke F, Oschkinat H, Reif B (2003) H-1 detection in MAS solid-state NMR Spectroscopy of biomacromolecules employing pulsed field gradients for residual solvent suppression. J Am Chem Soc 125:7788–7789

Chevelkov V, Rehbein K, Diehl A, Reif B (2006) Ultrahigh resolution in proton solid-state NMR spectroscopy at high levels of deuteration. Angew Chem Int Ed 45:3878–3881

Ferguson N, Becker J, Tidow H, Tremmel S, Sharpe TD, Krause G, Flinders J, Petrovich M, Berriman J, Oschkinat H, Fersht AR (2006) General structural motifs of amyloid protofilaments. Proc Natl Acad Sci USA 103:16248–16253

Franks WT, Wylie BJ, Schmidt HLF, Nieuwkoop AJ, Mayrhofer RM, Shah GJ, Graesser DT, Rienstra CM (2008) Dipole tensor-based atomic-resolution structure determination of a nanocrystalline protein by solid-state NMR. Proc Natl Acad Sci USA 105:4621–4626

Gardner KH, Rosen MK, Kay LE (1997) Global folds of highly deuterated, methyl-protonated proteins by multidimensional NMR. Biochemistry 36:1389–1401

Garrett DS, Seok YJ, Liao DI, Peterkofsky A, Gronenborn AM, Clore GM (1997) Solution structure of the 30 kDa N-terminal domain of enzyme I of the *Escherichia coli* phosphoenolpyruvate:sugar phosphotransferase system by multidimensional NMR. Biochemistry 36:2517–2530

Hennig M, Bermel W, Schwalbe H, Griesinger C (2000) Determination of psi torsion angle restraints from (3)J(C-alpha, C-alpha) and 3 J(C-alpha, H-N) coupling constants in proteins. J Am Chem Soc 122:6268–6277

Huber M, Hiller S, Schanda P, Ernst M, Bockmann A, Verel R, Meier BH (2011) A proton-detected 4D solid-state NMR experiment for protein structure determination. ChemPhysChem 12:915–918

Jaroniec CP, MacPhee CE, Astrof NS, Dobson CM, Griffin RG (2002) Molecular conformation of a peptide fragment of transthyretin in an amyloid fibril. Proc Natl Acad Sci USA 99:16748–16753

Kalbitzer HR, Leberman R, Wittinghofer A (1985) H-1-NMR spectroscopy on elongation-factor Tu from *Escherichia coli*—resolution enhancement by Perdeuteration. FEBS Lett 180:40–42

Laage S, Marchetti A, Sein J, Pierattelli R, Sass HJ, Grzesiek S, Lesage A, Pintacuda G, Emsley L (2008) Band-selective 1H–13C cross-polarization in fast magic angle spinning solid-state NMR spectroscopy. J Am Chem Soc 130:17216–17217

Lange A, Luca S, Baldus M (2002) Structural constraints from proton-mediated rare-spin correlation spectroscopy in rotating solids. J Am Chem Soc 124:9704–9705

Lemaster DM, Richards FM (1988) NMR sequential assignment of escherichia-coli thioredoxin utilizing random fractional Deuteriation. Biochemistry 27:142–150

Leppert J, Heise B, Ohlenschlager O, Gorlach M, Ramachandran R (2003) Broadband RFDR with adiabatic inversion pulses. J Biomol NMR 26:13–24

Levitt MH, Kolbert AC, Bielecki A, Ruben DJ (1993) High-resolution H-1-NMR in solids with frequency-switched multiple-pulse sequences. Solid State Nucl Mag 2:151–163

Linser R, Chevelkov V, Diehl A, Reif B (2007) Sensitivity enhancement using paramagnetic relaxation in MAS solid-state NMR of perdeuterated proteins. J Magn Reson 189:209–216

Linser R, Fink U, Reif B (2008) Proton-detected scalar coupling based assignment strategies in MAS solid-state NMR spectroscopy applied to perdeuterated proteins. J Magn Reson 193:89–93

Linser R, Fink U, Reif B (2010) Narrow carbonyl resonances in proton-diluted proteins facilitate NMR assignments in the solid-state. J Biomol NMR 47:1–6

Linser R, Dasari M, Hiller M, Higman V, Fink U, Lopez Del Amo JM, Markovic S, Handel L, Kessler B, Schmieder P, Oesterhelt D, Oschkinat H, Reif B (2011) Proton-detected solid-state NMR spectroscopy of fibrillar and membrane proteins. Angew Chem Int Ed Engl 50:4508–4512

Liu YJ, Zhao DQ, Altman R, Jardetzky O (1992) A systematic comparison of 3 structure determination methods from NMR data—dependence upon quality and quantity of data. J Biomol NMR 2:373–388

Marion D, Wuthrich K (1983) Application of phase sensitive two-dimensional correlated spectroscopy (Cosy) for measurements of H-1-H-1 spin–spin coupling-constants in proteins. Biochem Bioph Res Co 113:967–974

Paulson EK, Morcombe CR, Gaponenko V, Dancheck B, Byrd RA, Zilm KW (2003) Sensitive high resolution inverse detection NMR spectroscopy of proteins in the solid state. J Am Chem Soc 125:15831–15836

Reif B, van Rossum BJ, Castellani F, Rehbein K, Diehl A, Oschkinat H (2003) Characterization of H-1-H-1 distances in a uniformly H-2, N-15-labeled SH3 domain by MAS solid-state NMR spectroscopy. J Am Chem Soc 125:1488–1489

Sakellariou D, Lesage A, Hodgkinson P, Emsley L (2000) Homonuclear dipolar decoupling in solid-state NMR using continuous phase modulation. Chem Phys Lett 319:253–260

Schanda P, Huber M, Verel R, Ernst M, Meier BH (2009) Direct detection of (3 h)J(NC ‘) hydrogen-bond scalar couplings in proteins by solid-state NMR spectroscopy. Angew Chem Int Ed 48:9322–9325

Shaka AJ, Keeler J, Frenkiel T, Freeman R (1983) An improved sequence for broad-band decoupling—Waltz-16. J Magn Reson 52:335–338

van Rossum BJ, Castellani F, Rehbein K, Pauli J, Oschkinat H (2001) Assignment of the nonexchanging protons of the alpha-spectrin SH3 domain by two- and three-dimensional H-1-C-13 solid-state magic-angle spinning NMR and comparison of solution and solid-state proton chemical shifts. Chembiochem 2:906–914

Vinogradov E, Madhu PK, Vega S (1999) High-resolution proton solid-state NMR spectroscopy by phase-modulated Lee-Goldburg experiment. Chem Phys Lett 314:443–450

Vuister GW, Bax A (1992) Resolution enhancement and spectral editing of uniformly C-13-enriched proteins by homonuclear broad-band C-13 decoupling. J Magn Reson 98:428–435

Wasmer C, Lange A, Van Melckebeke H, Siemer AB, Riek R, Meier BH (2008) Amyloid fibrils of the HET-s(218–289) prion form a beta solenoid with a triangular hydrophobic core. Science 319:1523–1526

Wei DX, Akbey U, Paaske B, Oschkinat H, Reif B, Bjerring M, Nielsen NC (2011) Optimal H-2 rf pulses and H-2-C-13 cross-polarization methods for solid-state H-2 MAS NMR of perdeuterated proteins. J Phys Chem Lett 2:1289–1294

Wickramasinghe NP, Parthasarathy S, Jones CR, Bhardwaj C, Long F, Kotecha M, Mehboob S, Fung LW, Past J, Samoson A, Ishii Y (2009) Nanomole-scale protein solid-state NMR by breaking intrinsic 1HT1 boundaries. Nat Methods 6:215–218

Zech SG, Wand AJ, McDermott AE (2005) Protein structure determination by high-resolution solid-state NMR spectroscopy:

application to microcrystalline ubiquitin. J Am Chem Soc 127: 8618–8626

Zhou DH, Rienstra CM (2008) High-performance solvent suppression for proton detected solid-state NMR. J Magn Reson 192:167–172

Zwahlen C, Gardner KH, Sarma SP, Horita DA, Byrd RA, Kay LE (1998) An NMR experiment for measuring methyl–methyl NOEs in C-13-labeled proteins with high resolution. J Am Chem Soc 120:7617–7625